

## Strain-shift coefficients for phonons in $\text{Si}_{1-x}\text{Ge}_x$ epilayers on silicon

D. J. Lockwood\* and J.-M. Baribeau

*Institute for Microstructural Sciences, National Research Council, Ottawa, Canada K1A 0R6*

(Received 7 August 1991)

The measurement of the strain coefficients for the three longitudinal-optical phonons in strained  $\text{Si}_{1-x}\text{Ge}_x$  ( $0 < x < 0.35$ ) molecular-beam-epitaxy-grown epilayers on (100) Si is reported. Strain in the epilayers was varied by annealing metastable pseudomorphically grown epilayers at various temperatures and was measured by double-crystal x-ray diffractometry. The strain-shift coefficients for the phonons were obtained from Raman-scattering measurements of the annealed specimens. For all compositions it was found that the Si-Si phonon frequencies vary linearly with strain. The strain-shift coefficient, however, showed a small composition dependence, varying from about  $-750 \text{ cm}^{-1}$  at  $x = 0.08$  to about  $-950 \text{ cm}^{-1}$  at  $x = 0.35$ , corresponding to a stress factor  $\tau \approx 0.4 + 0.57x + 0.13x^2 \text{ cm}^{-1}/\text{kbar}$  for this vibration. The magnitude of the corresponding coefficients for the Si-Ge and Ge-Ge lines are slightly less than that of the Si-Si line, and vary in a similar way with  $x$ .

### I. INTRODUCTION

Raman-scattering spectroscopy has proved to be a versatile and nondestructive tool for measuring the physical properties of semiconductor superlattices.<sup>1</sup> Measurements of, for example, the acoustic and optic phonons in  $\text{Si}/\text{Si}_{1-x}\text{Ge}_x$  strained-layer superlattices can provide information on the layer thicknesses, composition, and strain.<sup>2,3</sup> In measuring the strain, attention is given to the shift of the optic-phonon frequencies away from their values in the bulk material. In Si layers only one Raman peak is observed due to the optic phonon at  $520 \text{ cm}^{-1}$  in bulk Si, whereas in  $\text{Si}_{1-x}\text{Ge}_x$  layers three peaks are found near 300, 400, and  $500 \text{ cm}^{-1}$  due to optic modes labeled as Ge-Ge, Si-Ge, and Si-Si, respectively.<sup>4</sup> The frequencies of the Si-Si and Ge-Ge lines in the alloy vary almost linearly with concentration, while the Si-Ge line exhibits a cusplike variation in its frequency.<sup>4-8</sup> In determining the strain in Si or  $\text{Si}_{1-x}\text{Ge}_x$  superlattice layers from the optic-phonon frequency, the strain-shift coefficient  $b$  (in  $\text{cm}^{-1}$ ) or stress factor  $\tau$  ( $\text{cm}^{-1}/\text{kbar}$ ) must be known for the material involved. Values for these parameters have been obtained for pure Si (or pure Ge) from a number of uniaxial stress experiments,<sup>9-14</sup> but the corresponding numbers for  $\text{Si}_{1-x}\text{Ge}_x$  are less well known.<sup>15,16</sup> It is not known, for example, how  $b$  varies precisely with  $x$  in the alloy for any of the three modes. Such information, however, is essential if Raman measurements are to be used routinely for accurate intralayer strain measurements in  $\text{Si}/\text{Si}_{1-x}\text{Ge}_x$  superlattices.

We have carried out measurements of strain, using x-ray diffraction, and the optic-phonon frequencies in a variety of  $\text{Si}_{1-x}\text{Ge}_x$  strained epilayers grown on (100)Si for Ge concentrations in the range  $0 < x < 0.35$ , as a preliminary study of this type on two epilayers had shown that the shifts of the Raman frequency and the x-ray Bragg peak are directly correlated.<sup>17,18</sup> The biaxial compressive strain in the layers was varied by annealing the samples. Analysis of the data thus obtained has en-

abled us to deduce the strain-shift coefficient for the Si-Si line over this concentration range and for the other two lines at higher- $x$  values. In the next section we describe the sample preparation method and experimental techniques used in this study. The results obtained are presented in Sec. III and analyzed for the parameters  $b$  and  $\tau$  in Sec. IV. Some conclusions are presented in the final section.

### II. EXPERIMENT

The epitaxial layers were grown by molecular-beam epitaxy (MBE) in a VG Semicon V80 system under optimized growth conditions.<sup>19</sup> All samples were grown at  $\sim 450^\circ\text{C}$  on lightly doped ( $1 \times 10^{15} \text{ cm}^{-3}$ ) 100-mm (100)Si wafers. The thickness of the various layers was chosen so that pseudomorphic growth could be preserved at the growth temperature. Physical data from the various samples are given in Table I. The uniformity in thickness and composition from the center to the edge of the wafer is estimated to be better than 1%. Sample G, which has the highest Ge concentration, was capped with a Si layer to increase the critical thickness for relaxation. Nevertheless, as compared with the others, which had a dislocation density less than  $5 \times 10^3$ , this sample showed a high defect density, presumably due to its high degree of strain. Wafer samples ( $1 \text{ cm}^2$ ) taken from adjacent locations were annealed (rapid thermal anneal in nitrogen in a Heatpulse 210 or vacuum anneal) between 500 and  $950^\circ\text{C}$  to induce partial relaxation of the built-in strain.

X-ray diffraction was used to determine the thickness and germanium fraction  $x$  of the as-grown epilayers and to measure the residual strain in annealed specimens. The measurements were performed with a BEDE 150 double-crystal diffractometer using the (400) reflection from a (100)Si monochromator crystal and  $\text{Cu } K\alpha$  radiation ( $\Lambda = 1.54 \text{ \AA}$ ). In this setup, the sampling area is estimated to be about  $0.2 \text{ cm}^2$ . The physical parameters given in Table I were obtained by dynamical simulation<sup>21</sup> of the rocking curves from the as-grown specimens. The

TABLE I. Physical data for the various  $\text{Si}_{1-x}\text{Ge}_x$  epilayers investigated in this work. Expressions for the effective stress are given in Ref. 20.

Sample	Thickness (nm)	$x$ ( $\pm 0.005$ )	Effective stress (GPa)	Remark
A	190 $\pm$ 10	0.208	0.72	smooth surface
B	160 $\pm$ 5	0.200	0.68	smooth surface
C	105 $\pm$ 5	0.286	0.97	textured surface
D	620 $\pm$ 10	0.079	0.28	textured surface
E	105 $\pm$ 5	0.124	0.34	smooth surface
F	180 $\pm$ 5	0.200	0.69	smooth surface
G	100 $\pm$ 10	0.35	1.1	200-nm Si cap, $3 \times 10^6$ defects/cm $^{-2}$

Ge concentrations obtained from the simulations were corrected to account for the well-known deviation from Vegard's law in the Si-Ge alloy system. The lattice constant  $a(x)$  in a  $\text{Si}_{1-x}\text{Ge}_x$  layer was approximated by the relationship

$$a(x) = 0.5431 + 0.02x + 0.0026x^2 \text{ (nm)}, \quad (1)$$

deduced from the data of Ref. 22.

The Raman spectra of the epilayers were recorded at 295 K in a quasibackscattering geometry using 300 mW of argon laser light at 457.9 nm for excitation. The measurements were performed on the same specimens used for the x-ray experiments, and in both experiments care was taken to position the probe within 1 mm from the center of the MBE specimen. In the Raman experiments the sampling area was approximately  $0.1 \times 1 \text{ mm}^2$ . The peak positions of the optic phonons were computer determined using a peak-finding algorithm.<sup>23</sup> The peaks were generally located to within  $\pm 0.1 \text{ cm}^{-1}$  by this procedure, although the absolute accuracy of any given peak frequency is limited to  $\pm 0.4 \text{ cm}^{-1}$  due to the spectrometer error. For the Si-Si line, greater absolute accuracy was obtained by using the Si-substrate Raman line as a reference point for determining the Si-Si line shifts. Repeated measurements of the Si-substrate line gave an average value of  $520.0 \text{ cm}^{-1}$  for its frequency, and so this value was assumed in determining the Si-Si line positions. By this means, the Si-Si line frequencies were found to within  $\pm 0.1 \text{ cm}^{-1}$  in all epilayers except for sample *D* where the epilayer was too thick for the Si substrate line to be observed.

### III. EXPERIMENTAL RESULTS

#### A. Double-crystal x-ray diffraction

In pseudomorphic epitaxial growth, the unit cell of the epilayer is tetragonally distorted to accommodate the lattice mismatch between the epilayer and underlying substrate material. The lattice strain  $\epsilon_{\perp}$  in the growth direction is related to the in-plane mismatch  $\epsilon_{\parallel}$  by the relationship

$$\epsilon_{\perp} = -[2\nu/(1-\nu)]\epsilon_{\parallel}, \quad (2)$$

where  $\nu$  is Poisson's ratio [ $\sim 0.279$  for Si and Ge (Ref. 24)] and  $\epsilon_{\parallel} = (a_{\text{sub}} - a_{\text{epi}})/a_{\text{epi}}$  is the lattice mismatch be-

tween the epilayer ( $a_{\text{epi}}$ ) and substrate ( $a_{\text{sub}}$ ) materials. Pseudomorphic growth can be maintained up to a critical thickness, above which it is energetically favorable to form misfit dislocations at the substrate/epilayer interface. Pseudomorphicity above the critical thickness can, however, be maintained if the layer is grown at sufficiently low temperature so that relaxation becomes kinetically limited. The activation energy barriers for nucleation and propagation of misfit dislocations then prevent the structure from reaching its equilibrium fully relaxed state. Such a structure is, however, highly metastable, and will start to relax if energy is supplied to the system via annealing above the growth temperature.

All the  $\text{Si}_{1-x}\text{Ge}_x$  epilayers investigated in this work were metastable, and partial relaxation, to various degrees, was achieved by annealing treatments. The strain in the epilayers was obtained by measuring the relative position  $\Delta\theta$  of the Bragg (400) x-ray-diffraction peak originating from the epilayer with respect to the fixed substrate reflection  $\theta_{\text{Si}}$ . The perpendicular strain  $\epsilon_{\perp}$  is given by

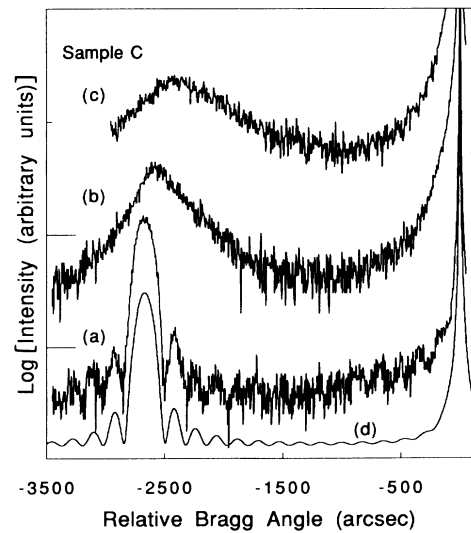


FIG. 1. (400) rocking curves from sample *C* (a) as-grown and after annealing 3 min at (b) 800°C and (c) 950°C. Curve (d) is a dynamical simulation of the as-grown sample obtained using the structural parameters given in Table I.

$$\varepsilon_{\perp} = \frac{\Lambda}{2a(x)\sin(\theta_{\text{Si}} + \Delta\theta)} - 1. \quad (3)$$

Figure 1 compares the (400) rocking curves from sample C as grown and after annealing 3 min at 800 and 950 °C. In Fig. 1 the simulated rocking curve (d) for the as-grown specimen is also displayed. Excellent agreement is found when the epilayer is simulated by a 105-nm alloy layer of composition  $x=0.286$ . In particular, the absence of broadening of the main epilayer diffracted peak at  $-2670$  arcsec and the observation of well-defined *Pendelossung* fringes indicates, respectively, that there is no significant variation in Ge concentration along the growth direction and that the substrate epilayer interface is well defined. Partial strain relaxation in the annealed specimens is revealed by the shift of the epilayer Bragg reflection toward the substrate reflection. The shift is generally accompanied by a broadening of the diffraction peak. This is due to the presence of threading dislocations in the epilayer and to local tilting of the lattice planes due to misfit dislocation segments propagating along the wafer surface.<sup>17</sup> This broadening reduces the accuracy in the determination of  $\Delta\theta$  for the most-relaxed specimens to about  $\pm 50$  arcsec.

### B. Raman-scattering measurements

Representative results from the Raman studies of the epilayers are shown for sample C in Fig. 2. The spectrum from the as-grown specimen [curve (a)] exhibits three main peaks attributed to scattering from longitudinal-optical phonons corresponding largely to vibrations of the Ge-Ge ( $\sim 300$   $\text{cm}^{-1}$ ), Si-Ge ( $\sim 400$   $\text{cm}^{-1}$ ), and Si-Si ( $\sim 500$   $\text{cm}^{-1}$ ) bonds in the alloy layer, and a strong peak due to the optical lattice vibration of the Si substrate ( $\sim 520$   $\text{cm}^{-1}$ ). Weaker optic-phonon lines near 255 and 435  $\text{cm}^{-1}$  have been attributed to a particular Si-Ge ordering within the alloy layer.<sup>25</sup> The effect of annealing on these spectral features can be seen in curves (b) and (c) of Fig. 2. This sample is one where the strain relaxation induced by annealing even at 950 °C is proportionally smaller than for other epilayers. Nevertheless, shifts of the Ge-Ge, Si-Ge, and Si-Si lines with strain relaxation were readily detected, as can be seen in Fig. 2. For example, these three lines move, respectively, from 293.6, 412.1, and 511.1  $\text{cm}^{-1}$  in the as-grown sample to 289.5, 408.9, and 508.3  $\text{cm}^{-1}$  in the sample annealed at 950 °C. The frequencies of the modes near 255 and 435  $\text{cm}^{-1}$  are remarkably insensitive to annealing, which is consistent with their assignment to a particular Si-Ge ordered state. For this reason, these modes were not included in the strain analysis. In the case of the Raman results, the precision of the measurement is not affected by line broadening at the higher anneal temperatures, as the Raman linewidths are not as sensitive to the presence of misfit dislocations as in the x-ray case.

### IV. DATA ANALYSIS

Following Anastassakis *et al.*,<sup>9</sup> when a strain is applied along the major axes of the cubic crystal, the triply degenerate optical mode near zero wave vector is split

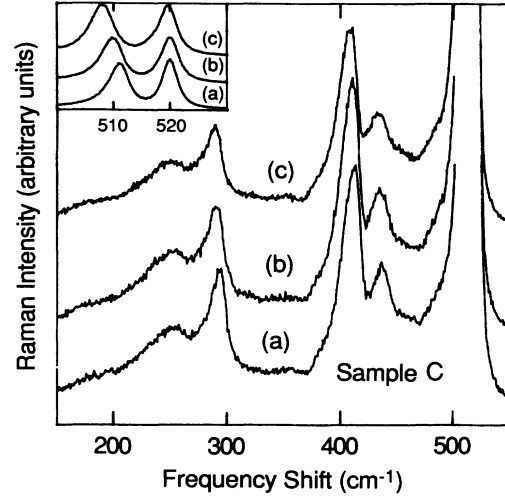


FIG. 2. Raman spectrum of sample C (a) as-grown and after annealing 3 min at (b) 800 °C and (c) 950 °C. The spectral resolution was 3.1  $\text{cm}^{-1}$ . The inset shows the 500- $\text{cm}^{-1}$  region of the spectrum recorded at a resolution of 1.6  $\text{cm}^{-1}$ .

into a singlet with wave vector parallel to the strain, and a doublet with wave vectors perpendicular to the strain direction. In a backscattering geometry only the singlet is observed, and the optical-phonon frequency  $\omega$  shifts according to the relationship

$$\omega = \omega_0 + \left(\frac{1}{2}\omega_0\right)(p\varepsilon_{\perp} + 2q\varepsilon_{\parallel}), \quad (4)$$

where  $\omega_0$  is the phonon frequency of the unstrained cubic lattice and  $p$  and  $q$  are phenomenological parameters. Equation (4) can be rewritten in terms of  $\varepsilon_{\parallel}$  using Eq. (2) to yield

$$\delta\omega = \omega - \omega_0 = \frac{1}{\omega_0} \left[ \frac{p\nu}{\nu-1} + q \right] \varepsilon_{\parallel} = b\varepsilon_{\parallel}. \quad (5)$$

In Eq. (5),  $b$  is the strain-shift coefficient relating the displacement of the phonon frequency with the lattice distortion in the plane of growth. The Raman shift  $\delta\omega$  is related to the change in the (400) Bragg reflection from the epilayer. Combining Eqs. (2), (3), and (5), and differentiating yields

$$\omega - \omega_0 \approx \frac{1}{2\omega_0} \left[ p + q\frac{\nu-1}{\nu} \right] \cot\theta_B (\Delta\theta_0 - \Delta\theta), \quad (6)$$

where  $\theta_B$  and  $\Delta\theta_0$  are, respectively, the Bragg angle and Bragg-angle shift relative to the substrate for the fully relaxed alloy. From Eq. (6) it is seen that the Raman shift varies linearly with the epilayer relative Bragg angle. In a plot of  $\omega$  versus  $\Delta\theta$ , assuming that  $p$  and  $q$  are not composition or strain dependent, values for  $b$  and for  $\omega_0$  are obtained from the slope  $m$  and from an extrapolation at  $\Delta\theta = \Delta\theta_0$ , respectively. In particular,  $b$  is given by

$$b = \left[ \frac{2\nu}{\nu-1} \right] m \tan\theta_B. \quad (7)$$

This result is illustrated in Fig. 3 for sample *G* for the Si-Si, Si-Ge, and Ge-Ge phonons. The vibration frequency for the three phonon modes exhibits a linear increase with the built-in strain. The strain-shift coefficient, for this sample, is practically identical for all modes and is about  $950 \text{ cm}^{-1}$ . The results obtained for sample *B* are shown in Fig. 4, where again it can be seen that the strain-shift coefficients are similar for all three modes. The trend with decreasing  $x$  is for the overall frequency shifts, when maximum strain relief due to annealing has occurred, of the Ge-Ge, Si-Ge, and Si-Si lines to remain comparable.

For the other samples the Si-Ge and Ge-Ge phonons were either weak and not well defined or the strain relaxation was relatively small, and an accurate strain shift could only be measured for the Si-Si vibration. The results are summarized in Fig. 5, which is a plot of the Si-Si frequency as a function of the relative Bragg angle. For all samples the phonon frequency varies linearly with the strain within the experimental uncertainties. It can be seen that the total amount of relaxation upon annealing varies from sample to sample. This is in part explained by the different effective stress<sup>20</sup> that exists within each

sample (see Table I). The effective stress is the residual force responsible for creation and propagation of misfit dislocations. Anomalies are observed, however (sample *D*, in particular, should exhibit a slower relaxation), and this may be explained by a variation in the number of heterogeneous dislocation nucleation sites, which are also known to favor relaxation in strained epitaxy.<sup>26</sup> Variation in the surface morphology in some samples (see Table I) suggests that differences may exist in the density of dislocation sources.

The Si-Si phonon frequency for unstrained  $\text{Si}_{1-x}\text{Ge}_x$  was obtained from extrapolation of the straight lines of Fig. 5 at  $\Delta\theta_0$ . Figure 6 compares the results obtained from the various epilayers to bulk measurements by Brya.<sup>5</sup> The three measurements<sup>4,5,7</sup> of the  $x$  dependence of the bulk alloy Si-Si line frequency resulted in three different slopes; Brya's results were chosen for comparison purposes here because they gave the median slope. Except for a constant shift of  $1.3 \text{ cm}^{-1}$ , which probably originates from a different calibration of the frequencies, the results of both studies are in remarkable agreement. This indicates that the extrapolation procedure used in some of the linear fits shown in Fig. 5 is a reasonable one.

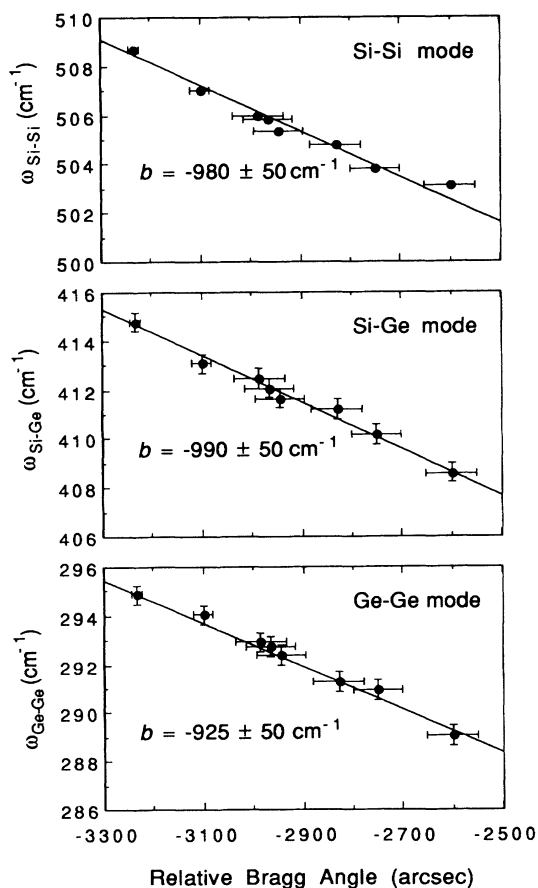


FIG. 3. (a) Si-Si (b) Si-Ge, and (c) Ge-Ge phonon frequencies as a function of relative Bragg angle from sample *G* with various residual strains.

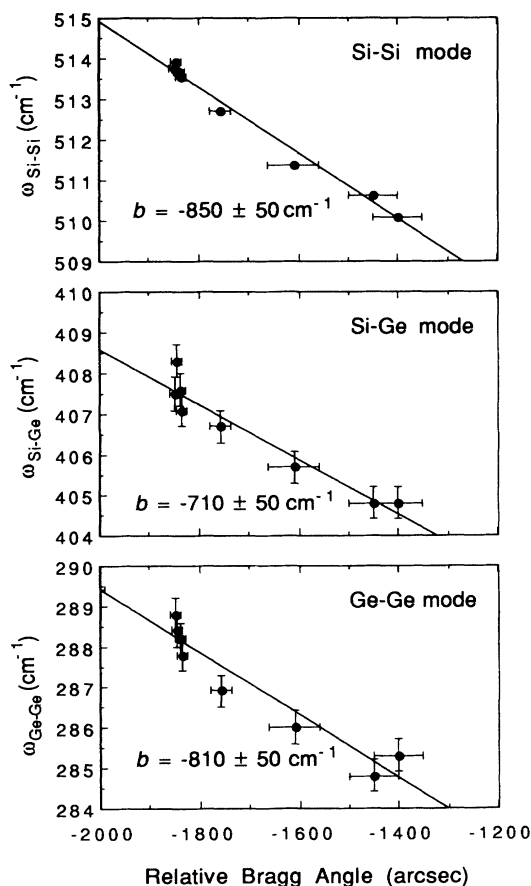


FIG. 4. (a) Si-Si (b) Si-Ge, and (c) Ge-Ge phonon frequencies as a function of relative Bragg angle from sample *B* with various residual strains.

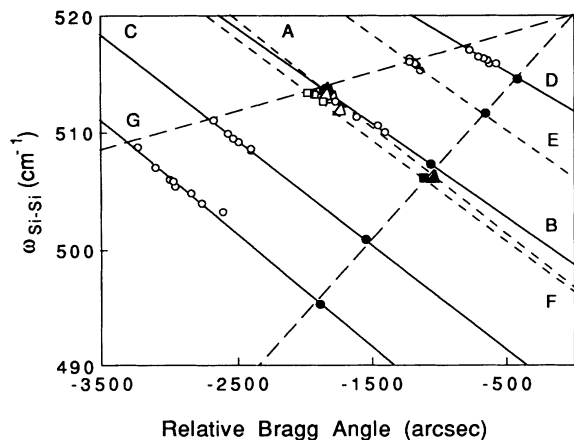


FIG. 5. Si-Si phonon frequency as a function of relative Bragg angle for different  $\text{Si}_{1-x}\text{Ge}_x$  epilayers and with various residual strains. Points in black are extrapolated values for a fully relaxed epilayer. The long dashed lines represent  $\omega_{\text{Si-Si}}$  vs  $\Delta\theta$  for a fully strained and fully relaxed epilayer. The solid lines are best linear fits obtained from the experimental data only; the short dashed lines are the best linear fits obtained including the extrapolated frequency for a fully relaxed epilayer.

The Raman strain-shift coefficient as obtained from the slope determinations shown on Fig. 5 is plotted in Fig. 7 as a function of Ge concentration. Despite the fairly large uncertainties involved in its determination, a definite increase in the magnitude of  $b$  with Ge fraction is observed. The extrapolated value for pure Si is about  $-715 \text{ cm}^{-1}$ , in excellent agreement with the value of  $-723 \text{ cm}^{-1}$  deduced from two earlier uniaxial pressure studies (see Table II). There is a considerable difference, however, between our extrapolated  $b$  value for pure Si

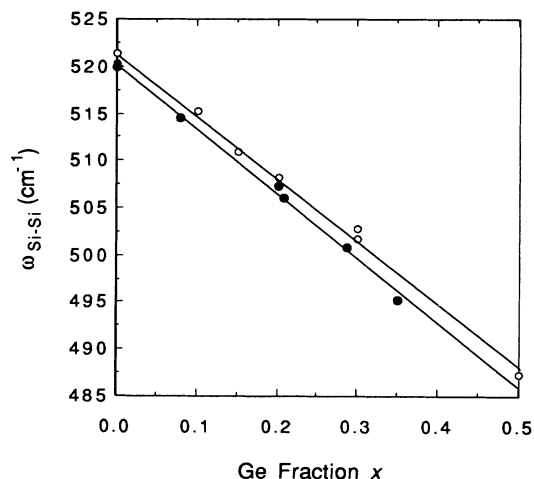


FIG. 6. Frequency of the Si-Si longitudinal phonon in the  $\text{Si}_{1-x}\text{Ge}_x$  alloy as a function of germanium concentration  $x$ . Open symbols are from the work of Brya (Ref. 5), closed symbols were obtained from extrapolation of the frequency dependence of partially relaxed epilayers (Fig. 5) to the value corresponding to full relaxation. The solid lines are best linear fits to the data.

TABLE II. Values for the parameters  $p$  and  $q$  and for the strain coefficient  $b$  in Si and Ge determined at photon wavelength  $\lambda$ .

Material	$p$ ( $10^{28} \text{ s}^{-2}$ )	$q$ ( $10^{28} \text{ s}^{-2}$ )	$b$ ( $\text{cm}^{-1}$ )	$\lambda$ (nm)
Si	$-1.43^a$	$-1.89^a$	$-723$	647
Si	$-1.2^b$	$-1.8^b$	$-723$	633
Si	$-1.76^c$	$-2.22^c$	$-832$	1064
Si			$-715^d$	458
Ge	$-0.47^e$	$-0.62^e$	$-408$	488

<sup>a</sup>Reference 11.

<sup>b</sup>Reference 9.

<sup>c</sup>Reference 13.

<sup>d</sup>Present work.

<sup>e</sup>Reference 10.

and the most recent determination ( $b = -832 \text{ cm}^{-1}$ ) in Table II. The reason for this difference seems to lie in the wavelengths used to excite the Raman spectra. As Anastassakis, Cantarero, and Cardona<sup>13</sup> have already pointed out, there is a 10–30% difference in the phonon deformation potentials obtained in bulk materials, depending on whether or not the material is transparent at the exciting wavelength. As Table II shows, the smaller values for  $b$  are obtained at shorter wavelengths, where Si is strongly absorbing. The implication for bulk Si is that there is some relaxation of the applied stress near the surface, which the shorter wavelengths are probing.<sup>13</sup> In our experiments, our excitation wavelength is well above the bulk Si band gap, and yet in all but one case the incident and scattered light penetrate right through the epilayer. Thus the surface relaxation effect is not a likely explanation.

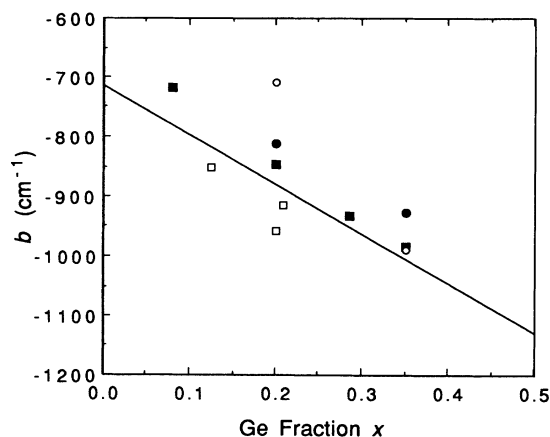


FIG. 7. Strain coefficients for  $\text{Si}_{1-x}\text{Ge}_x$  epilayers as a function of germanium concentration  $x$ . The solid and open squares are values for the Si-Si mode deduced from slope measurements in Fig. 5 excluding and including extrapolated bulk values, respectively. In the former case, the uncertainty on the  $b$  value is estimated to be about  $\pm 50 \text{ cm}^{-1}$ , in the latter case it is about  $\pm 100 \text{ cm}^{-1}$ . The solid line is a best linear fit  $b = -715 - 825x$  ( $\text{cm}^{-1}$ ). Solid and open circles are discrete values of  $b$  for the Ge-Ge and Si-Ge modes, respectively, as deduced from Figs. 3 and 4.

tion for our smaller  $b$  magnitude and may not be the correct explanation in the bulk Si case, either. The value at  $x \approx 0.2$  is also in good agreement with results from Halliwell *et al.*,<sup>16</sup> who found that  $b = -930 \pm 90 \text{ cm}^{-1}$  for  $x < 0.2$ , although they reported no variation in  $b$  with  $x$ . Our somewhat-limited results for the Si-Ge and Ge-Ge line  $b$  values shown in Fig. 7 are not too different from the Si-Si line case, and they all vary with Ge concentration. For the Si-Ge line Cerdeira *et al.*<sup>15</sup> determined that  $b = -455 \text{ cm}^{-1}$  for  $x < 0.65$ , which is considerably different from our result (see Fig. 7) and is closer to that for pure Ge (see Table II). Cerdeira *et al.* obtained their  $b$  value for the Si-Ge mode from a linear fit to their  $\delta\omega$  versus  $x$  data, which is not the same as our procedure and results in a constant (average)  $b$  value independent of  $x$ . Our  $\delta\omega$  versus  $x$  results are shown in Fig. 8, where  $\delta\omega$  is determined for the Si-Si line from the data of Fig. 5 and for the Si-Ge and Ge-Ge lines from the differences between the mode frequencies in a fully strained epilayer and the corresponding bulk alloy frequencies estimated from the results of Brya.<sup>5</sup> Our results are in qualitative agreement with the experimental results of Cerdeira *et al.* (see Fig. 8) in that there are no major differences between the behaviors of the three modes for  $x < 0.35$ , and in both cases the Si-Ge and Ge-Ge lines have a similar but slightly weaker  $x$  dependence than the Si-Si line. However, our results exhibit a stronger concentration dependence in  $\delta\omega$  for all three lines, which suggests that the incommensurate single alloy layers used by Cerdeira *et al.* as references for the zero-strain frequencies of the lines (see Ref. 15) were in fact partially strained. Residual strain is known to exist in  $\text{Si}_{1-x}\text{Ge}_x$  epilayers grown well above the critical thickness.<sup>27</sup>

Equation (5) may be rewritten for bulk materials in terms of the interfacial biaxial stress  $\sigma$  to yield<sup>28</sup>

$$\delta\omega = b(S_{11} + S_{12})\sigma = \tau\sigma, \quad (8)$$

where  $S_{11}$  and  $S_{12}$  are the compliance constants and  $\tau$  is the stress factor. An approximate value for the Si-Si mode stress factor for a  $\text{Si}_{1-x}\text{Ge}_x$  alloy layer can be obtained from interpolation of the compliance constants of pure Si and Ge (Ref. 24) and using the linear fit of Fig. 7. This yields for  $\tau$  the expression

$$\tau \approx 0.4 + 0.57x + 0.13x^2 \text{ (cm}^{-1}\text{/kbar)}, \quad (9)$$

which may be used for low-Ge concentration ( $x < 0.35$ ).

## V. CONCLUSIONS

This study of strain relaxation in  $\text{Si}_{1-x}\text{Ge}_x$  epilayers grown pseudomorphically on (100)Si using Raman and x-ray techniques has enabled us to determine the strain-shift coefficient  $b$  of the three optic phonons in the alloy for  $x < 0.35$ . The interesting result is that, contrary to the findings of earlier investigations, the  $b$  values for all three modes are very similar for a given  $x$  and increase linearly with increasing  $x$ . The coefficients for all three modes are clearly derived from the bulk-Si  $b$  value. Our extrapolated bulk-Si value is close to other determinations where the Raman excitation wavelengths lie above the band gap, but is quite different from the value obtained for a wavelength below the band gap. As the strain in the  $\text{Si}_{1-x}\text{Ge}_x$  epilayers is of a different type than that of simple uniaxial stress applied to bulk Si, the closeness of our extrapolated  $b$  value and bulk-Si literature values is noteworthy. It suggests that the surface-strain-relaxation effect invoked to explain the difference between  $b$  values obtained above and below band-gap excitation in bulk Si is probably not the correct one. The fact that our  $b$  values for the three modes at a given  $x$  are similar indicates that the epilayer substrate, and hence the in-plane lattice constant, is the dominant factor in determining their magnitude. It also indicates that the bulk Si and Ge values for the phonon deformation potentials  $p$  and  $q$  (and hence  $b$ ) cannot be used in some extrapolation procedure, as has been attempted previously,<sup>15</sup> for the  $\text{Si}_{1-x}\text{Ge}_x$  epilayer case. Conversely, our results cannot be used directly to estimate  $p$  and  $q$  values for the alloy: this must come from direct uniaxial pressure studies of the bulk alloys. It would be interesting to perform such studies to compare with our results, and to study  $\text{Si}_{1-x}\text{Ge}_x$  epilayers grown on Ge to see if the alloy phonon  $b$  coefficients are then related to the bulk-Ge  $b$  value.

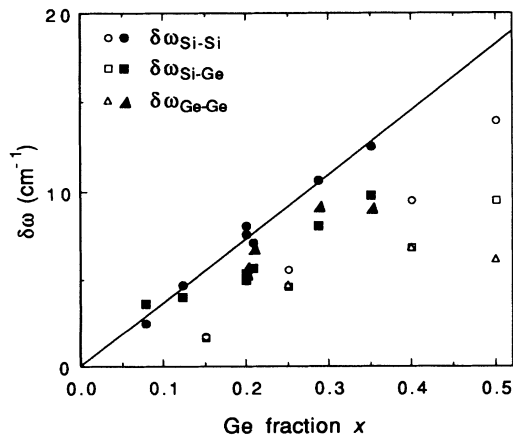


FIG. 8. Frequency difference  $\delta\omega$  for the three optic modes between peak positions in fully strained and fully relaxed (bulk)  $\text{Si}_{1-x}\text{Ge}_x$  epilayers as a function of Ge concentration. Closed symbols are from the present work using the frequencies of fully strained as-grown material and the bulk values from Fig. 6 for the Si-Si line and from Brya (Ref. 5) for the other lines. Open symbols are from Cerdeira *et al.* (Ref. 15).

## ACKNOWLEDGMENT

We are grateful to H. J. Labbé for expert technical assistance in the Raman measurements.

\*FAX: (613) 957-8734.

- <sup>1</sup>*Light Scattering in Semiconductor Structures and Superlattices*, edited by D. J. Lockwood and J. F. Young (Plenum, New York, 1991).
- <sup>2</sup>B. Jusserand and M. Cardona, in *Light Scattering in Solids V: Superlattices and Other Microstructures*, edited by M. Cardona and G. Güntherodt, Topics in Applied Physics Vol. 66 (Springer, Berlin, 1989), p. 49.
- <sup>3</sup>J. Sapriel and B. Djafari Rouhani, *Surf. Sci. Repts.* **10**, 189 (1989).
- <sup>4</sup>J. B. Renucci, M. A. Renucci, and M. Cardona, *Solid State Commun.* **9**, 1651 (1971).
- <sup>5</sup>W. J. Brya, *Solid State Commun.* **12**, 253 (1973).
- <sup>6</sup>G. M. Zinger, I. P. Ipatova, and A. V. Subashiev, *Fiz. Tekh. Poluprovodn.* **11**, 656 (1977) [*Sov. Phys. Semicond.* **11**, 383 (1977)].
- <sup>7</sup>T. Ishidate, S. Katagiri, K. Inoue, M. Shibuya, K. Tsuji, and S. Minomura, *J. Phys. Soc. Jpn.* **53**, 2584 (1984).
- <sup>8</sup>M. I. Alonso and K. Winer, *Phys. Rev. B* **39**, 10056 (1989).
- <sup>9</sup>E. Anastassakis, A. Pinczuk, E. Burstein, F. H. Pollack, and M. Cardona, *Solid State Commun.* **8**, 133 (1970).
- <sup>10</sup>F. Cerdeira, C. J. Buchenauer, F. H. Pollak, and M. Cardona, *Phys. Rev. B* **5**, 580 (1972).
- <sup>11</sup>M. Chandrasekhar, J. B. Renucci, and M. Cardona, *Phys. Rev. B* **17**, 1623 (1978).
- <sup>12</sup>T. Englert, G. Abstreiter, and J. Pontcharra, *Solid State Electron.* **23**, 31 (1980).
- <sup>13</sup>E. Anastassakis, A. Cantarero, and M. Cardona, *Phys. Rev. B* **41**, 7529 (1990).
- <sup>14</sup>Z. Sui, I. P. Herman, and J. Bevk, *Appl. Phys. Lett.* **58**, 2351 (1991).
- <sup>15</sup>F. Cerdeira, A. Pinczuk, J. C. Bean, B. Battlogg, and B. A. Wilson, *Appl. Phys. Lett.* **45**, 1138 (1984).
- <sup>16</sup>M. A. G. Halliwell, M. H. Lyons, S. T. Davey, M. Hockly, C. G. Tuppen, and C. J. Gibbings, *Semicond. Sci. Technol.* **4**, 10 (1989).
- <sup>17</sup>P. Y. Timbreil, J.-M. Baribeau, D. J. Lockwood, and J. P. McCaffrey, *J. Appl. Phys.* **67**, 6292 (1990); *J. Electron. Mater.* **19**, 657 (1990).
- <sup>18</sup>D. J. Lockwood and J.-M. Baribeau, in *Light Scattering in Semiconductor Structures and Superlattices* (Ref. 1).
- <sup>19</sup>J.-M. Baribeau, T. E. Jackman, P. Maigné, D. C. Houghton, and M. W. Denhoff, *J. Vac. Sci. Technol. A* **5**, 1898 (1987).
- <sup>20</sup>D. C. Houghton, *J. Appl. Phys.* **70**, 2136 (1991).
- <sup>21</sup>Simulation performed with RADS software, BEDE Scientific Instruments Ltd, Durham, UK.
- <sup>22</sup>J. P. Dismukes, L. Ekstrom, and R. J. Paff, *J. Phys. Chem.* **10**, 3021 (1964).
- <sup>23</sup>J. W. Arthur, *J. Raman Spectrosc.* **5**, 2 (1976).
- <sup>24</sup>M. Neuberger, *Handbook of Electronic Materials* (IFI Plenum, New York, 1971), Vol. 5.
- <sup>25</sup>D. J. Lockwood, K. Rajan, E. W. Fenton, J.-M. Baribeau, and M. W. Denhoff, *Solid State Commun.* **61**, 465 (1987).
- <sup>26</sup>D. D. Perovic, G. C. Weatherly, J.-M. Baribeau, and D. C. Houghton, *Thin Solid Films* **183**, 141 (1989).
- <sup>27</sup>H.-J. Herzog, H. Jorke, E. Kasper, and S. Mantl, in *Proceedings of the Second International Symposium on Silicon Molecular Beam Epitaxy*, edited by J. C. Bean and L. J. Schowalter (Electrochemical Society, Pennington, NJ, 1987), p. 58.
- <sup>28</sup>G. Abstreiter, H. Brugger, T. Wolf, R. Zachai, and C. Zeller, in *Two-Dimensional Systems: Physics and New Devices*, edited by G. Bauer, F. Kuchar, and H. Heinrich (Springer-Verlag, Berlin, 1986), p. 130.